Journal of Applied Polymer Science

Synergistic effect of graphene oxide-silver nanofillers on engineering performances of polyelectrolyte complex nanofiber membranes

Ning Cai,[1] Huan Zeng,[1] Jing Fu,[1] Vincent Chan,[2] Mei Chen,[1] Hui Li,[1] Faquan Yu [1]
[1]Key Laboratory for Green Chemical Process of Ministry of Education, Hubei Key Laboratory of Novel Reactor & Green Chemical Technology, School of Chemical Engineering and Pharmacy, Wuhan Institute of Technology, Wuhan 430073, China
[2]Department of Chemical Engineering, Khalifa University, Abu Dhabi 127788, UAE
Correspondence to: F. Yu (E-mail: fyuwucn@gmail.com)

ABSTRACT: The poor mechanical and antibacterial performance has become a big hurdle for extending the application of polyelectrolyte complex (PEC) nanofibers in various fields. In this study, chitosan/gelatin (CG) composite nanofiber system was used for portraying the synergistic enhancement of mechanical and antibacterial properties of PEC nanofiber membranes by inclusion of graphene oxide-silver (GO-Ag) nanofillers. In particular, the introduction of 1.5 wt % GO-Ag has raised the elastic modulus and tensile strength of CG nanofiber membrane by 105% and 488%, respectively, which are partially attributed to the alleviated restacking of graphene sheets by the anchored AgNPs. Meanwhile, the diameters of inhibition zone against *Escherichia coli* and *Staphylococcus aureus* on LB-agar plates induced by GO-Ag/CG nanofiber membranes are increased by 80.5% and 50.1%, respectively, compared to that by CG membrane. The synergistic improvement of antimicrobial performance of GO-Ag/CG may be related to the accumulation of microorganisms induced by GO. In summary, the incorporation of GO-Ag composite nanofillers has emerged as an effective strategy for engineering PEC nanofiber membranes for potential applications in nanomedicine and tissue engineering. © 2018 Wiley Periodicals, Inc. J. Appl. Polym. Sci. **2018**, *135*, 46238.

KEYWORDS: electrospinning; fibers; membranes; mechanical properties; polyelectrolytes

Received 25 October 2017; accepted 5 January 2018
DOI: 10.1002/app.46238

INTRODUCTION

Polyelectrolyte complex (PEC) represents a novel class of macromolecular materials formed by the association of polycation and polyanion.[1] The formation of PEC is mainly driven by the electrostatic attraction although other intra- or inter-molecular forces including hydrogen bonding and van der Waals forces may also play minor roles in the complexation.[1] Because PEC generally contains two distinctive polyelectrolytes, PEC offers competitive advantages in its physicochemical properties over either one of its constituent polyelectrolytes. When PEC was fabricated into one-dimensional (1D) or two-dimensional (2D) nanostructures, that is, nanofibers, such type of PEC system possessed superior properties including high specific area and porosity compared to its counterparts in other forms.[2–4] Recently, PEC nanofibers have been exploited for potential applications in various fields including nanomedicine, environmental technology and drug delivery.[2] For instance, Jiang *et al.* fabricated chitosan/sodium alginate PEC nanofiber membranes as biomaterial scaffolds for potential tissue engineering applications.[5] In addition, Meng *et al.* specifically designed poly(diallyldimethylammonium chloride)/poly(4-styrenesulfonic acid) PEC nanofiber membranes for the use in water purification.[6]

In the areas of regeneration medicine and food packaging, antibacterial property which is generally absent in conventionally designed PEC nanofibers is highly desirable for combating pathogens and contaminants.[7–9] For instance, wound dressing made of PEC nanofiber membranes should possess excellent antibacterial activity to target pathogenic bacteria and to prevent wound infection, leading to the achievement of practical wound healing.[10] The limited antibacterial ability of PEC has become a major hurdle for the realization of PEC-based technology in biomedicine. Thus, the design and development of various classes of PEC membranes with enhanced antibacterial properties have attracted the increasing attentions.[11–14] In addition, mechanical properties play a vital role in the durability and compliance of PEC nanofiber membranes/scaffolds for long-term biomedical applications *in vivo*.[15] As such, satisfactory mechanical performance of nanofiber based biomaterial scaffolds are indispensable to the success of tissue regeneration by providing an favorable microenvironment for cell adhesion, proliferation, migration and differentiation.[3] Due to high porosity and weak inter-fiber cohesion, PEC nanofiber membranes usually do not meet the basic requirements in the mechanical properties for *in vivo* implementation.[16] For instance, Young's

modulus CS/GE nanofiber membranes is capped at 37.9 MPa even after extensive optimization of the fabrication procedures, which is significantly lower than that of human skin (83 MPa).[17] Based on the aforementioned factors, both antibacterial and mechanical properties of conventional PEC nanofiber membrane are posed for serious reengineering in order to warrant the applications of PEC nanofibers in biomedicine.

The introduction of reinforcement agents is a popular way to enhance the mechanical properties of polymeric nanofibers. Different types of nanofillers such as graphene oxide (GO),[17] nanodiamonds,[18] carbon nanotube,[19] and halloysite nanotube,[20] have been used to fabricate composite nanofibers. Particularly, GO demonstrated the outstanding performance for reinforcing chitosan/gelatin (CS/GE) PEC nanofiber system. Attributed to the effective filler-matrix interaction, the addition of only 1.5 wt % of GO filler has led to 358% elevation in the tensile strength.[17] Furthermore, a number of antibacterial compounds, antibiotics and nanofillers can be incorporated into PEC nanofiber membranes for rendering the material with antibacterial activity.[9,21,22] For example, silver nanoparticles (AgNPs) are well known for their excellent antibacterial activity and are incorporated in a number of commercial products.[23–25] Although the presence of antibacterial activity in GO is still under active debate,[26,27] GO-Ag nanocomposites, synthesized by the growth of AgNPs on GO surface, have been reported to demonstrate significant enhancement on antibacterial activity compared with the simple mixture of individual GO and AgNPs.[28] At the same time, the decoration GO with AgNPs effectively inhibits the restacking of graphene sheets,[29] which is beneficial for the improvement of mechanical performance of polymeric composite materials.[30] In light of the outstanding mechanical properties of GO and antibacterial properties of AgNPs, the incorporation of GO-Ag nanocomposites may simultaneously enhance the critical engineering performances including antibacterial activity and mechanical strength of PEC nanofiber membranes.

Currently, limited research has been focused on the formulation of new strategies to improve mechanical and antibacterial properties of PEC nanofibers. This work aims to explore the feasibility of improving the mechanical and antibacterial properties of PEC nanofiber membranes with the incorporation of GO-Ag nanocomposites during the fabrication process. Firstly, CG PEC which has been thoroughly characterized was chosen as the model PEC system for our study herein. GO-Ag nanocomposites were synthesized by *in situ* reduction of Ag^+ on the surface of GO sheets. Then the GO-Ag/CG nanofiber membranes were produced from GO-Ag/CG mixture in 90 wt % acetic acid through electrospinning technique. Secondly, transmission electron microscopy (TEM), ultraviolet–visible (UV–vis) spectra, X-ray diffraction (XRD), energy-dispersive X-ray spectroscopy (EDS), Fourier transform infrared (FTIR) spectroscopy were employed to verify the deposition of AgNPs on the surface of GO. The morphology and structure of the electrospun nanofiber membranes were examined by scanning electron microscopy (SEM), TEM, and FTIR. Moreover, the mechanical properties of GO-Ag/CG nanofiber membranes were evaluated by standard tensile tests. Lastly, the antibacterial properties of GO-Ag/CG nanofiber membranes were investigated with agar disc diffusion method by using Gram-negative *Escherichia coli* and Gram-positive *Staphylococcus aureus* as two model microorganisms. Overall, this study shed light on the promising effect of GO-Ag nanofillers on the improvement of mechanical and antibacterial properties of PEC nanofiber membranes.

EXPERIMENTAL

Materials

Chitosan ($M_w = 100$ kDa, degree of deacetylation = 90%, $M_w/M_n = 1.8$, purity 98%) was obtained from Zhejiang Golden-shell Biochemical, China. Gelatin, acetic acid, sodium citrate, and silver nitrate were purchased from Sinopharm Chemical Reagent, China. GO was synthesized by oxidizing pristine graphite powder following a modified Hummers' method.[31] All chemicals are analytical grade and used without further purification.

Preparation of AgNPs and GO-Ag Nanocomposites

GO-Ag nanocomposites were synthesized by using sodium citrate as the reducing agent. The schematic procedure was show in Scheme 1. In brief, 6 mg mL^{-1} of GO suspension mixed with 3 mg mL^{-1} of $AgNO_3$ (the weight ratio of GO/Ag^+ ions = 1:1). The solution was heated at 90 °C, and then sodium citrate solution (0.1 wt %) was added dropwise to the reaction mixture which was kept at 90 °C for 1.5 h. The product was collected by centrifugation and then washed five times with deionized water. AgNPs were prepared with similar approach by using the same weight of $AgNO_3$ as precursor in the absence of GO. All products were freeze-dried to remove water for subsequent electrospinning and characterization.

Fabrication of Electrospun CG-Based Nanofiber Membranes

GO-Ag/CG nanofiber membranes with 1.5 wt % GO-Ag loading were prepared by electrospinning, as illustrated in Scheme 1. In brief, GO-Ag dispersion (1 mg mL^{-1}, aqueous solution) and CS solution (20 mg mL^{-1}, 2 wt % acetic acid) were mixed in equal volume and stirred for 24 h at room temperature. Subsequently, the GO-Ag functionalized with CS was collected by centrifugation. Acetic acid solution (90 wt %) were continuously supplied to dissolve the sediment remained after centrifugation followed by ultrasonication for obtaining CS functionalized GO-Ag suspension. Afterwards, CS and GE powders were dissolved in the GO-Ag suspension by stirring of 1 h for preparing 15 and 20 wt % solutions, respectively. The electrospinning precursor solution for 1.5 wt % GO-Ag/CG nanofibers was finally obtained by mixing the CS and GE solutions containing GO-Ag mentioned above homogeneously at CS:GE weight ratio of 1:1. Afterwards, the electrospinning process was conducted by an apparatus comprised of the following parts: a syringe pump, a high voltage DC power supply, and a vertical metal plate for collecting nanofibers. A 10 mL syringe with electrospun precursor solution was linked to a stainless needle. The needle tip was set up horizontally. The electrospinning parameters were adjusted as follows: DC voltage, 24 kV; collecting distance between needle tip and the collector, 10 cm; feeding rate, 0.7 mL h^{-1}; relatively humidity, 30%–40%; temperature, 25 °C. Following electrospinning process, all nanofiber membranes were peeled off from the aluminum foil and dried under vacuum in order to remove the solvent residues for further characterization. As the weight fraction of GO and Ag in GO-Ag is 51% and 49% (determined by EDS analysis in Morphological and Structural Properties of

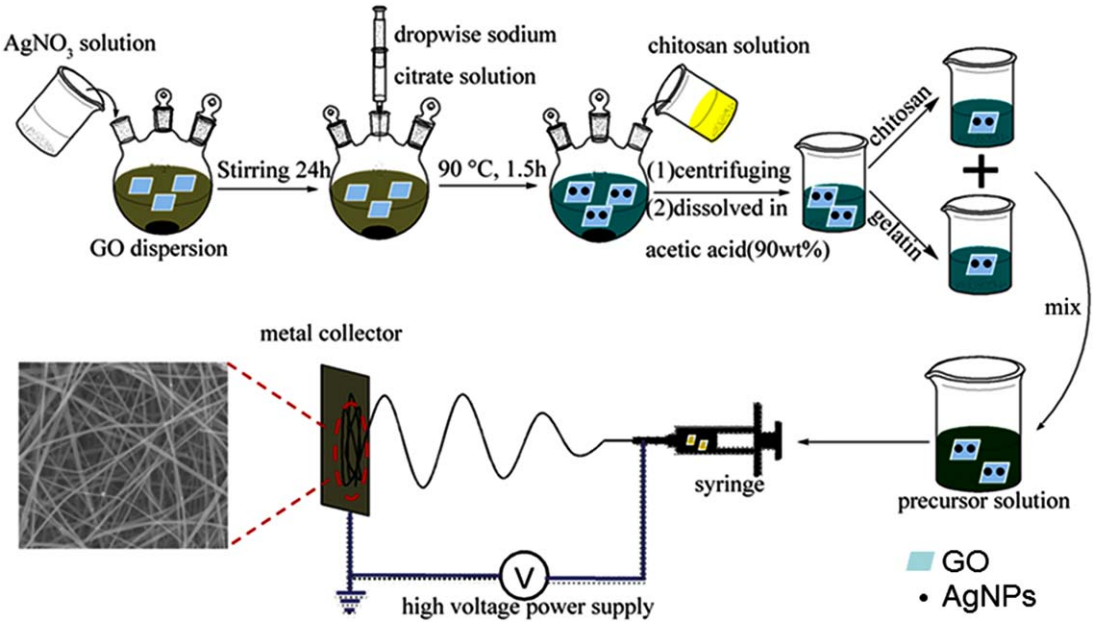

Scheme 1. Schematic illustration of the fabrication of electrospun GO-Ag/CG nanofiber membranes. [Color figure can be viewed at wileyonlinelibrary.com]

GO-Ag Nanocomposites section), the control samples of nanofiber membranes, GO/CG composite nanofibers with 0.765 wt % GO loading, AgNPs/CG with 0.735 wt % AgNPs loading, GO + Ag/CG with 0.765 wt % GO and 0.735 wt % AgNPs loading, were prepared using the similar procedure describe above. The concentration of CG in electrospinning solution for all CG-based nanofibers is kept to be 17.14 wt %.

Characterization

Morphology, crystal phase, and structure of GO-Ag nanocomposites were examined by TEM (JEOL JEM-2100), XRD (Bruker D8 Advance) and FTIR spectroscopy (Perkin Elmer Spectrum Two). UV–vis (Shimadzu UV-1650PC) spectrometer and EDS (JEOL JSM-5510LV) were used to investigate the composition of GO-Ag nanocomposites. The morphology of CG-based nanofibers and the dispersion of incorporated fillers were examined by SEM (Hitachi TM3030) and TEM, respectively. Chemical structure, the crystal structure, and thermal property of CG-based nanofibers were characterized by FTIR, and XRD and differential scanning calorimetry (DSC, Seiko Instruments, DSC 6220), respectively.

Mechanical Testing

The mechanical behaviors of CG-based nanofiber membranes were investigated according to ASTM D882–09 by a tensile testing machine (MTS systems, CMT8202) equipped with a 200 N load cell. The thickness of nanofiber membrane was measured with micrometer. All CG-based nanofiber membranes were cut into 60 mm × 5 mm of strips and then pulled at a speed of 10 mm min^{-1} with a 40 mm original gauge length. Each sample was tested for at least five times to obtain the mean value.

Antibacterial Activities

The antibacterial activity of CG-based nanofiber membranes were evaluated by the agar disc diffusion method. *E. coli* (ATCC 25922) and *S. aureus* (ATCC 25923) were used as model microorganisms herein. Bacteria were cultured overnight at 37 °C in Luria-Bertani (LB) broth under orbital shaker under 150 rpm. After incubation, the bacteria were diluted to a concentration of 10^6 CFU mL^{-1} and spread onto LB-agar plates. CG-based nanofiber membranes were sterilized and punched to obtain circular discs with the diameter of 6 mm, and are then gently laid on selected region of the inoculated plates. After the incubation at 37 °C for 24 h, inhibitory zones were determined by measuring the clear area formed around each circular sample. All the experiments were carried out in triplicate to obtain the mean value.

To investigate the influence of CG-based nanofiber membranes on the growth kinetics of *E. coli* and *S. aureus*, colorimetric method was used. The bacterial suspension (concentration of 10^8 CFU mL^{-1}) was inoculated in 10 mL of LB broth containing different CG-based nanofiber membranes with dimensions of 1 cm × 3 cm. After incubation at 37 °C under continuous shaking at 200 rpm, bacterial growth kinetics was evaluated by measuring the optical density (OD) at 600 nm every 30 min. All the experiments were carried out in triplicate and the mean values were obtained.

Statistical Analysis

All the data were shown as a mean ± standard deviation. A one-way analysis of variance (ANOVA) was performed to compare the mean values among different groups. Statistical significance was tested at $P < 0.05$.

RESULTS AND DISCUSSION

Morphological and Structural Properties of GO-Ag Nanocomposites

The morphology of AgNPs and GO-Ag nanocomposites were first examined by TEM. As shown in Figure 1(a), AgNPs have the typical spherical morphology. For GO-Ag, the circular AgNPs are uniformly scattered throughout the GO sheets

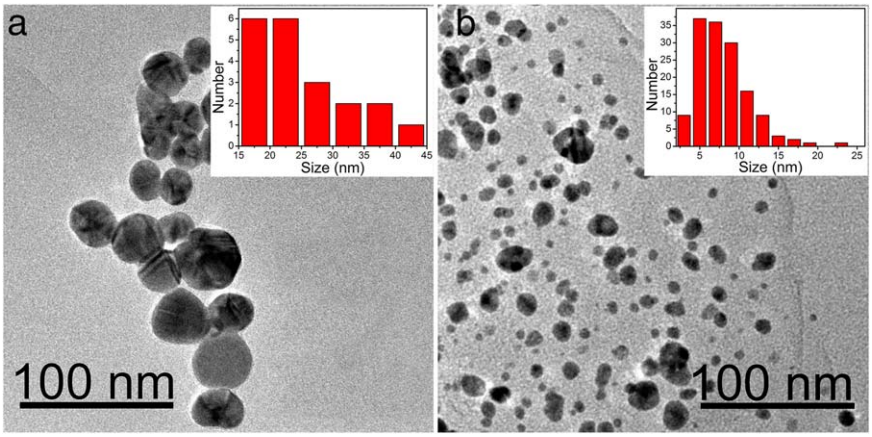

Figure 1. TEM images of (a) AgNPs and (b) GO-Ag nanocomposites. [Color figure can be viewed at wileyonlinelibrary.com]

[Figure 1(b)]. The pristine AgNPs were prepared through the reduction of Ag^+ with the aid of sodium citrate as the reductant and stabilizer. The synthesis of GO-Ag nanocomposites is relied on the binding of Ag^+ ions to the oxygen-containing groups of the GO sheets, which provides nucleation sites for the anchoring and growth of AgNPs. By analyzing the TEM images of the two samples, the averaged diameter of AgNPs on the GO sheets was 8.0 ± 0.8 nm, which is obviously lower than that of pristine AgNPs (25.2 ± 0.7 nm). When GO sheets rather than pristine AgNPs act as supporting material during the synthesis of GO-Ag, the presence of GO nucleation sites inhibits the aggregation of anchored AgNPs and eventually leads to the reduction in size of AgNPs immobilized on GO sheets.[32]

The chemical properties of GO, AgNPs, and GO-Ag nanocomposites were also characterized by UV–vis spectra. As shown in Figure 2(a), GO exhibited a strong absorption band at approximately 230 nm corresponding to π-π* aromatic transitions of C = C bonds, and a shoulder band at 300 nm due to π-π*

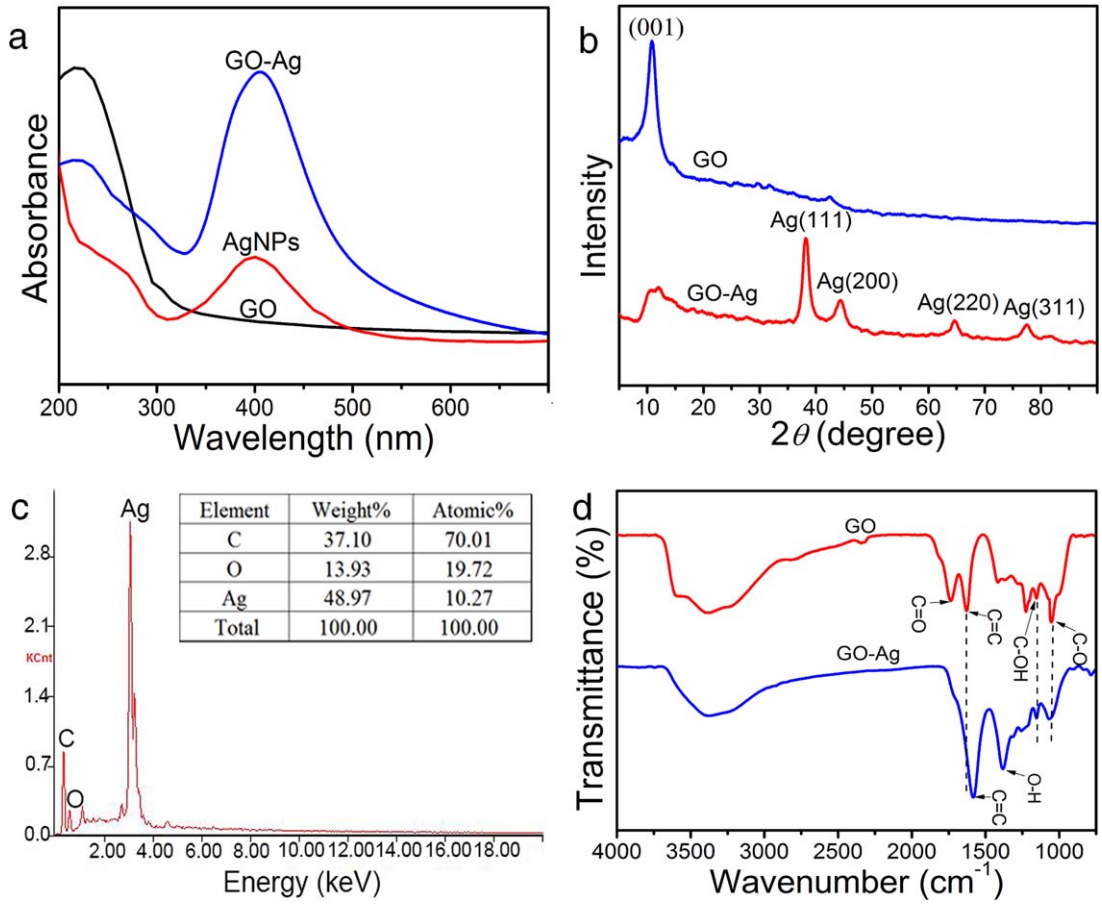

Figure 2. (a) UV–vis spectrum of GO, AgNPs and GO-Ag nanocomposites, (b) XRD patterns of GO and GO-Ag nanocomposites, (c) EDS spectrum of GO-Ag nanocomposites, and (d) FTIR spectra of GO and GO-Ag nanocomposites. [Color figure can be viewed at wileyonlinelibrary.com]

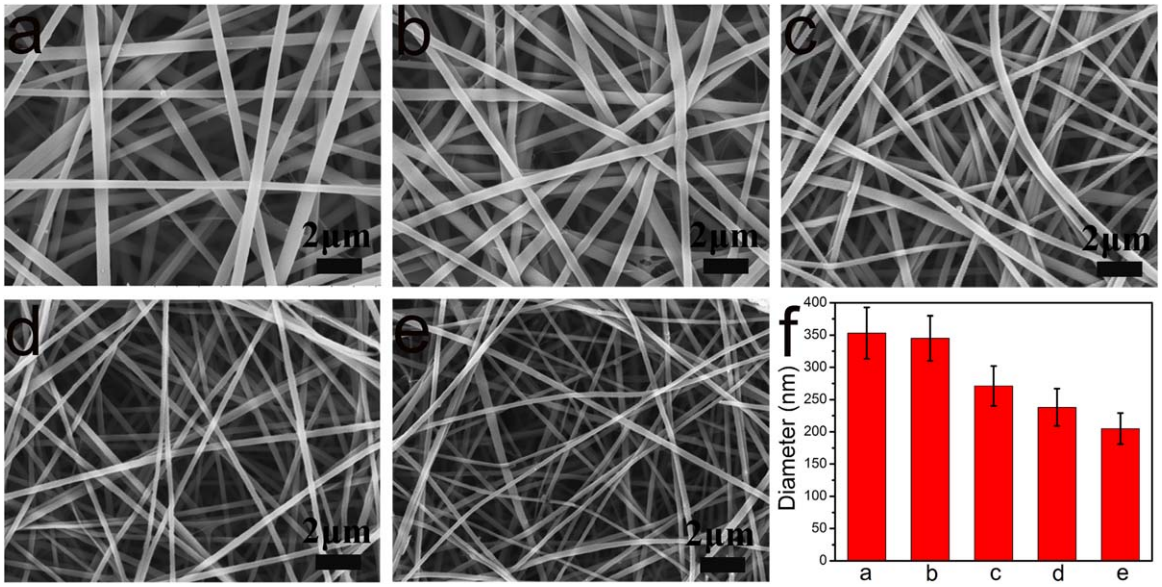

Figure 3. SEM images of (a) CG, (b) AgNPs/CG, (c) GO/CG, (d) GO + Ag/CG, (e) GO-Ag/CG nanofiber membranes, and (f) the mean diameter of CG-based nanofibers. [Color figure can be viewed at wileyonlinelibrary.com]

electronic transitions of C═O bonds. AgNPs showed a strong adsorption band at ~400 nm, corresponding to the Ag plasmon resonance.[33] This distinctive Ag plasmon resonance band was also observed at ~410 nm in the adsorption spectrum of GO-Ag, indicating AgNPs were successfully deposited on the GO sheets. It is reported that the redshift in plasmon resonance band may be ascribed to the shrinkage of AgNPs,[34] which is in agreement with the TEM results mentioned above.

The crystal structure of GO and GO-Ag was examined by XRD. In Figure 2(b), GO displayed a sharp (001) diffraction peak at $2\theta = 10.5°$, in accordance with the previous report.[35] For GO-Ag, the characteristic peak of GO at $2\theta = 10.5°$ still existed but its intensity was significantly reduced. It is because GO crystal face is likely masked by the facile formation of AgNPs.[36] In addition, the GO-Ag displayed additional diffraction peaks at $2\theta = 38.3°$, 44.2°, 64.6°, and 77.5°, which were assigned to the (111), (200), (220), and (311) crystalline planes of face-centered cubic silver (JCPDS file no. 07–0783),[29] confirming the existence of Ag in GO-Ag nanocomposites. From EDS analysis of GO-Ag [Figure 2(c)], the synthesized GO-Ag nanocomposites contained about 48.97 wt % silver element, 13.93 wt % oxygen element, and 37.10 wt % carbon element. The result as mentioned above strongly validated the distinctive chemical composition of GO-Ag compared to GO.

FTIR spectra of GO and GO-Ag nanocomposites were shown in Figure 2(d). GO displays the characteristic peaks located at 1733, 1628, 1230, and 1065 cm^{-1}, corresponding to C═O stretching vibrations, C═C skeletal vibration of the graphene sheets, C—OH stretching vibrations and C—O stretching vibrations of alkoxy groups, respectively.[37,38] Following the immobilization of AgNPs, the peak at 1733 cm^{-1} vanished and the peak ascribed to the skeletal vibration of the graphene sheets shifted from 1628 to 1582 cm^{-1}, which was likely induced by the interactions between AgNPs and GO sheets.[39] Moreover, the intensity of the peak at 1380 cm^{-1} ascribed to O—H (carboxyl) deformation vibration for GO-Ag was significantly higher than that for GO, which is likely to stem from surface-bound sodium citrate. This finding clearly confirms that the sodium citrate moieties are attached to the surface of GO-Ag, which stabilizes GO-Ag in solution during synthesis process.[40]

Morphological and Structural Properties of CG-Based Nanofiber Membranes

The morphology of CG-based nanofiber membranes were characterized by SEM. As shown in Figure 3(a–e), the surface of all types of CG-based nanofibers was rather smooth without visible beaded structure. However, as illustrated in Figure 3(f), the CG-based nanofibers possessed different diameters, which were 353 ± 40 nm for CG, 345 ± 35 nm for AgNPs/CG, 271 ± 31 nm for GO/CG, 238 ± 29 nm for GO + Ag/CG and 205 ± 24 nm for GO-Ag/CG. Therefore, the addition of nanofillers induced the shrinkage of CG nanofibers. It is reported that the low viscosity and high electrical conductivity of electrospun solution is beneficial for the formation of thinner nanofibers.[41] As listed in Table I, electrical conductivity and viscosity of electrospinning solutions showed increasing trend against the addition of different fillers (from 185 ± 3 mPa s and 2.88 ± 0.07 μS cm^{-1} for pristine CG to 265 ± 2 mPa s and 6.97 ± 0.13 μS cm^{-1} for GO-Ag/CG). The

Table I. Electrical Conductivity (σ) and Viscosity (μ) of CG-Based Electrospinning Solution

Sample	σ (μS/cm)	μ (mPa s)
CG	2.88 ± 0.07	185 ± 3
AgNPs/CG	2.91 ± 0.05	186 ± 2
GO/CG	5.58 ± 0.09	248 ± 2
GO + Ag/CG	6.64 ± 0.11	260 ± 3
GO-Ag/CG	6.97 ± 0.13	265 ± 2

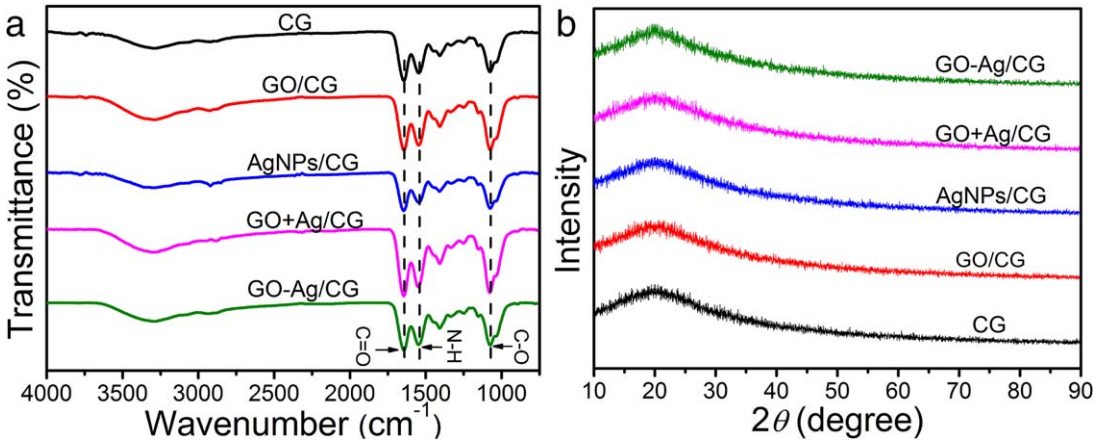

Figure 4. (a) FTIR spectra and (b) XRD patterns of CG-based nanofiber membranes. [Color figure can be viewed at wileyonlinelibrary.com]

trend mentioned above demonstrated that the larger extend due to the increase of electrical conductivity of CG upon GO-Ag addition played a more important role in determining the final size of electrospun CG-based nanofibers. Similar shrinkage of nanofibers following the addition of nanofillers have also been reported in nanodiamond/poly(vinyl alcohol) (PVA), montmorillonite/CS/PVA, and GO/PVA/CS systems.[42–44]

FTIR measurement was performed to study the interactions between the nanofillers and composite matrix. As shown in Figure 4(a), characteristic peaks of CG nanofiber membranes displayed at 1640, 1540, and 1065 cm^{-1}, which were attributed to the stretching vibration of —C═O, bending vibration of N—H and stretching vibration of —C—O—C— groups, respectively.[45] As the formation of CG PEC is mainly driven by electrostatic attraction between NH_3^+ of chitosan and COO^- of gelatin, the intensity ratio of the two peaks at 1640 and 1540 cm^{-1} can partially reflect the degree of polyelectrolyte complexation for CG PEC.[15] The intensity ratio of the CG-based nanofibers incorporated with different nanofillers were almost maintained at the same value (1.472 ± 0.008), implying no discernable disruption of the intermolecular interaction between CS and GE was detected upon the addition of fillers.

To examine the influence of different nanofillers on the crystalline structure of CG composites, XRD was performed. As shown in Figure 4(b), all XRD patterns of CG-based composites were similar among all samples and just a single band was identified at $2\theta = 19.5°$, indicating their low crystallinity. In addition, there was only slight change in the scale and intensity of the diffraction band for CG-based composites, suggesting that the incorporation of low content of nanofillers did not produce the change of crystallinity of CG composite matrix. Moreover, nearly negligible effect of fillers on the crystallinity of composites has been found on GO/CS/GE and graphene/AgNPs/polypyrrole nanofibers.[17,46]

Thermal Properties of CG-Based Nanofiber Membranes

Thermal properties may be affected by the added nanofillers, which can be monitored by DSC. As illustrated in Figure 5, each DSC curve exhibits a characteristic endothermic peak which is ascribed to the evaporation of loosely bonded water and termed to be dehydration temperature (T_D).[47–49] No secondary peaks were observed in any CG-based nanofibers, indicating good miscibility of all samples and absence of phase separation despite of the presence of CS, GE, and different nanofillers. The elevation of T_D following the introduction of nanofillers indicated the improvement of thermal stability in the composite nanofiber. Moreover, GO-Ag/CG possessed the highest T_D at 111.5 °C among the five specimens, which was even 9.3 °C larger than that of GO + Ag/CG (102.2 °C). It is known that the improvement of thermal stability of polymer is tightly correlated to good dispersion state of nanofillers.[18] More significant improvement on CG by GO-Ag nanocomposites than by the mixture of nonassociated GO and AgNPs suggests the decoration of AgNPs can promote the exfoliation and dispersion of GO sheets in the composite matrix.

Mechanical Properties of CG-Based Nanofiber Membranes

The mechanical properties of the electrospun composite nanofiber membranes were investigated by the tensile stress–strain testing method. Representative stress–strain curves of the CG-based nanofiber membranes are presented in Figure 6(a). Moreover, the elastic modulus and tensile strength of all samples are

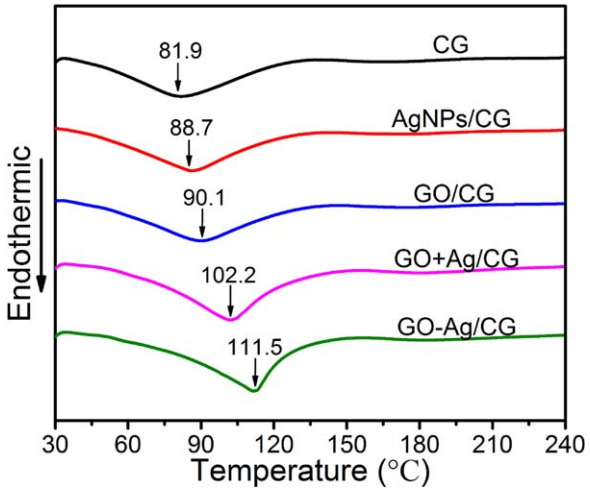

Figure 5. DSC curves of CG-based nanofiber membranes. [Color figure can be viewed at wileyonlinelibrary.com]

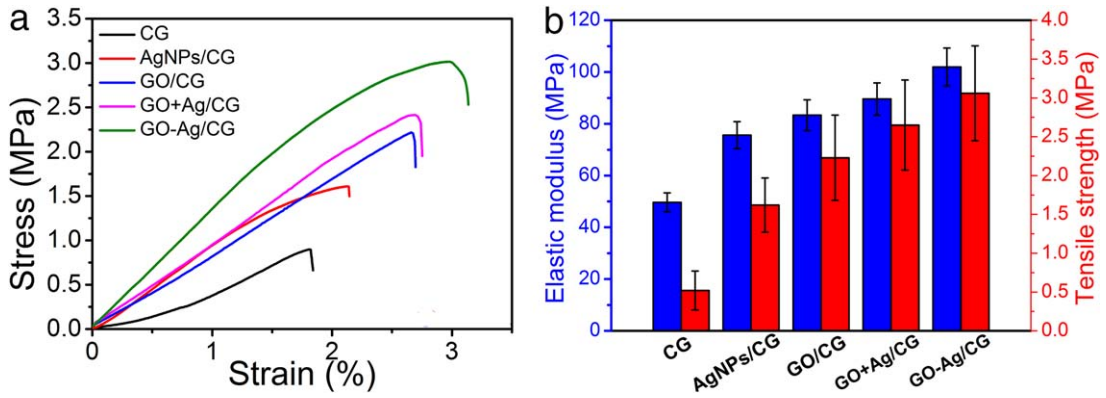

Figure 6. (a) The representative stress–strain curves and (b) tensile properties of CG-based nanofiber membranes. [Color figure can be viewed at wileyonlinelibrary.com]

presented in Figure 6(b). It was obvious that the addition of nanofillers improved elastic modulus and tensile strength. For CG samples, the elastic modulus and tensile strength are 49.7 and 0.52 MPa, respectively. With the incorporation of AgNPs to CG nanofiber membranes, the elastic modulus and tensile strength ascend to 75.6 and 1.62 MPa, indicating 52% and 211% increase, respectively. The addition of GO induces the respective 68% and 329% increase in the elastic modulus and tensile strength of CG composites matrix, respectively. Interestingly, the addition of both GO and AgNPs produces elastic modulus of 89.6 MPa and tensile strength of 2.58 MPa, meaning the respective 80% and 396% augment on GO + Ag/CG. Therefore, the addition of dual nanofillers (GO and AgNPs) can lead to better mechanical enhancement on CG than the addition of a single type of nanofillers (GO or AgNPs). It is interesting that the mechanical reinforcement effects of GO + Ag and GO-Ag on CG are different. The elastic modulus and tensile strength of GO-Ag/CG are even higher than those of GO + Ag/CG [Figure 6(b)], suggesting the GO decorated with AgNPs enhances mechanical properties of CG more effectively than GO + Ag (simple mixture of GO and AgNPs). Thus, the structure of nanofillers also tunes the mechanical properties of composites.

It is known that nanoparticles (i.e., silica, hydroxyapatite, metal, metal oxides, and other inorganic particles), tubular materials (i.e., carbon nanotube and halloysite nanotubes) and layered materials (i.e., graphene derivatives and layered silicate) can improve the mechanical strength of electrospun nanofiber membranes.[50–53] The effective mechanical enhancement does not work without efficient stress transfer from PEC nanofiber to nanofillers, which highly hinges on good dispersion and strong interactions between nanofillers and composite matrix.[44,54] However, nanofillers agglomerate can accelerate crack initiation, impairing mechanical performance of composite nanofibers. Thus, all nanofillers used in this study were treated by chitosan to improve their dispersion in 90 wt % acetic acid during the preparation of electrospinning solution. In fact, the incorporation of any of the four nanofillers (GO, AgNPs, GO + Ag, and GO-Ag) induced substantial improvement on the mechanical properties, supporting the effectiveness of this pretreatment step as mentioned above. As two dimensional sheets comprised of sp^2 carbon atoms, GO bears rich oxygen-containing functional groups such as hydroxyl and carboxyl. Thus, strong molecular interactions likely existed between GO and CG within the composites matrix. For example, GO can interact with chitosan through hydrogen bonding. Furthermore, electrostatic attraction occurs between deprotonated carboxylic groups of GO and protonated -NH_2 group of chitosan. In addition, the sheet-like form of GO endows high specific area to interact with CG composites matrix. Thus, high specific area and rich oxygen-containing functional groups contribute to the more conspicuous mechanical enforcement of CG composites matrix by GO than by AgNPs, as illustrated in Figure 6(b). When GO + Ag fillers (simple mixture of GO and AgNPs) was used to reinforce the mechanical properties of CG, better mechanical performance was demonstrated on GO + Ag/CG composites than that on either GO/CG or AgNPs/CG, demonstrating either GO or AgNPs played an important roles in improving the mechanical properties of CG nanofibers. If GO-Ag composite nanofillers with the same GO/Ag weight ratio as GO + Ag were employed, further mechanical enhancement on CG nanofibers was achieved. The elastic modulus and tensile strength of GO-Ag/CG nanofiber membranes are 102.0 and 3.06 MPa, achieving 13% and 19% increase compared with GO + Ag/CG, and 105% and 488% improvement compared with CG, respectively. It has been reported that the incorporation of two or more nanofillers together may synergistically enhance the mechanical properties of composites.[52] For PEC made of sodium carboxymethyl cellulose (CMC) and poly(2-methacryloyloxy ethyl trimethylammonium chloride) (PDMC), the tensile strength of 2 wt % GO-carbon nanotube (CNT)/PEC (1:1 in GO/CNT weight ratio) is 2.3, 1.6, and 4.8 times as high as those of CNT/PEC, GO/PEC, and pristine PEC membranes, respectively, which may be attributed to the formation of 3D network of GO nanosheets bridged by CNT.[55] In our study, the synergistical effect was also produced with the change of structure of added nanofillers. Although the exact mechanism responsible for this collective effect of multiple nanofillers on the mechanical enhancement of GO-Ag is not clear, it is believed that the AgNPs anchored on GO surface play a vital role. The decorated AgNPs on GO can act as molecular spacers to alleviate the restacking of graphene sheets and promote the effective dispersion of graphene sheets.[29]

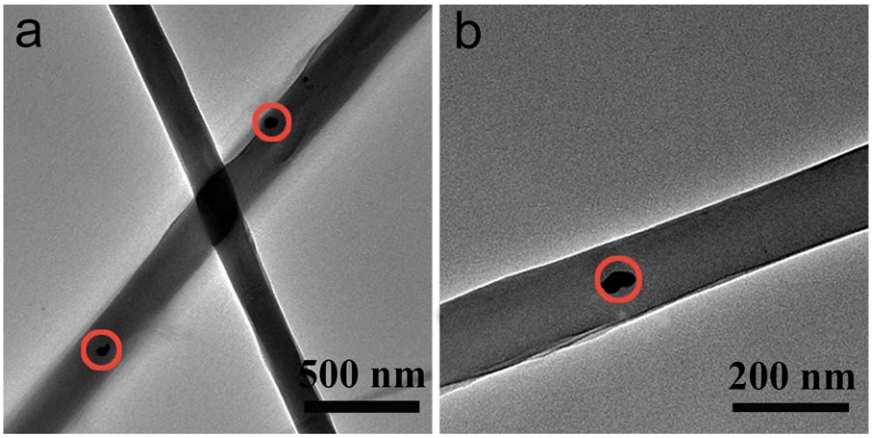

Figure 7. TEM images of GO-Ag/CG nanofiber. [Color figure can be viewed at wileyonlinelibrary.com]

As shown in Figure 7, no particle aggregations can be identified in GO-Ag nanocomposites by TEM observation. The well dispersed GO provides a larger surface area to interact with composite matrix, which is conducive to stress transfer from PEC matrix to GO-Ag fillers. Thus, GO-Ag hybrid nanofillers induced better improvement on the mechanical performance of CG nanofibers than simple mixture of GO and AgNPs fillers. In fact, similar synergistical effect of hybrid fillers on mechanical properties of polymer was also witnessed on GO-ZnO/poly(lactic acid) and GO-Ag/PVA composites.[56,57] Thus, GO-Ag is excellent candidate for improving the mechanical properties of PEC nanofibers for more demanding biomedical applications.

Antibacterial Properties of CG-Based Nanofiber Membranes

The antibacterial activities of the CG-based nanofiber membranes were evaluated by using agar disc diffusion method. As illustrated in Figure 8(a), the inhibitory zones against *E. coli* and *S. aureus* which clearly appeared on the region with the deposited CG nanofiber membranes, had a diameter of 8.34 mm and 8.02 mm, respectively. The pronounced antimicrobial ability of CG nanofibers is imparted by chitosan.[58] Chitosan can bind to the negatively charged surface of bacteria, which likely induces the leakage of intracellular constituents and inhibits the synthesis of RNA.[59] Correspondingly, the growth of bacteria was impeded. With the addition of GO, no apparent change in the diameter of inhibition zone are identified [Figure 8(b)], implying that the incorporation of GO into CG composites matrix did not induce the substantial improvement on its antibacterial performance. Despite the existence of toxicity of GO to bacteria reported in previous work,[26,60,61] limited or lack of antibacterial activity of GO was also observed,[62–64] which was in accordance with our results. In contrast to GO/CG, AgNPs/CG and GO + Ag/CG nanofiber membranes demonstrated enhanced antibacterial activities [Figure 8(c,d)], which were resulted from AgNPs. Although the antibacterial mechanisms of AgNPs are not fully elucidated, it is accepted that the damage of bacterial membrane induced by the direct contact of AgNPs and the generation of reactive oxygen species resulted from eluted Ag^{+} are responsible for the killing of bacteria.[65]

It is worth noting that the diameters of inhibitory zones against *E. coli* and *S. aureus* acquire their maximum values on GO-Ag/CG among five CG-based membranes, which are 80.5% and 50.1% larger than those of CG nanofiber membranes, respectively. Particularly, the inhibitory zones against *E. coli* and *S. aureus* of GO-Ag/CG nanofiber membranes are even larger than the respective one of GO + Ag/CG nanofiber membranes, despite the same chemical composition. This result implied that the remarkably enhanced antibacterial activities of GO-Ag nanocomposites were not simply the additive effects of the two

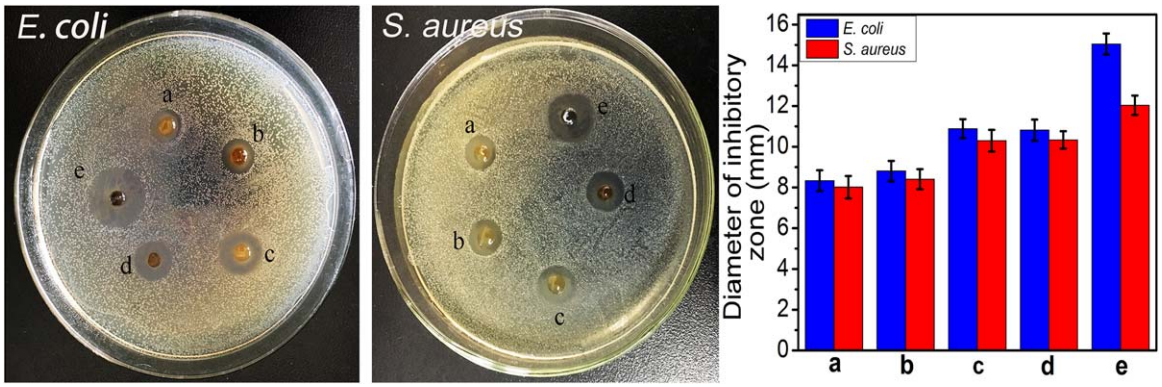

Figure 8. Bacteria (*E. coli* and *S. aureus*) inhibition zone of CG-based nanofiber membranes on LB-agar plates: (a) CG, (b) GO/CG, (c) AgNPs/CG, (d) GO + Ag/CG, and (e) GO-Ag/CG, and the diameter of inhibitory zone of CG-based nanofiber membranes. [Color figure can be viewed at wileyonlinelibrary.com]

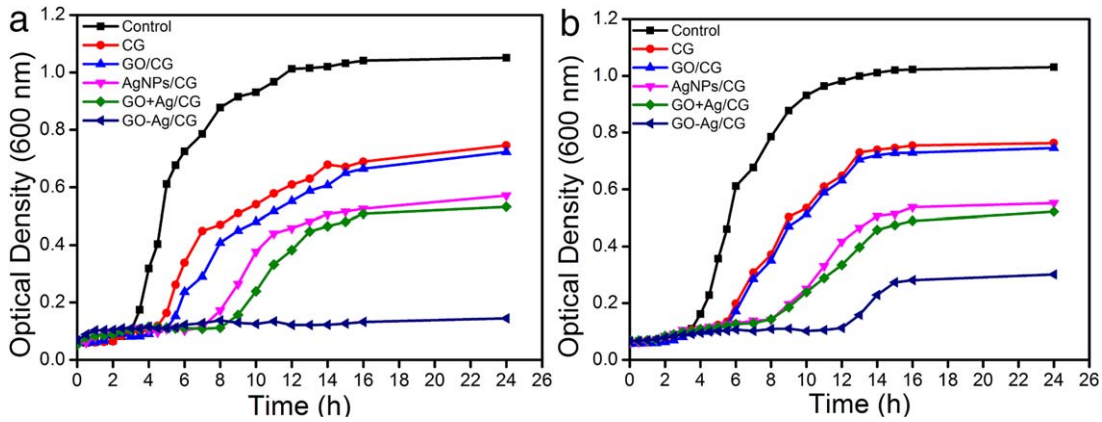

Figure 9. The growth curve of (a) *E. coli* and (b) *S. aureus* treated with CG-based nanofiber membranes. [Color figure can be viewed at wileyonlinelibrary.com]

components of nanofiller, GO and AgNPs, when they function independently. It is known that strong interactions can form between GO sheets and lipid bilayer of cell membranes due to hydrophobic property of sp^2 carbon of GO.[66] Therefore, GO surface can attract bacteria strongly. The bacteria accumulated by GO are just in the vicinity of AgNPs anchored on GO sheets. As a result, direct contact to AgNPs or exposure to high concentration of Ag^+ occurs easily, producing elevated antibacterial activity. In contrast, GO or AgNPs only exerted antibacterial activity independently in GO + Ag/CG, producing no synergistical effect. Because of the negligible antibacterial activity of GO in this study, it can be deduced that GO + Ag/CG possess the almost equivalent antibacterial ability to AgNPs/CG, which was verified by Figure 8(c,d). Thus, antibacterial properties of CG nanofiber membranes was enhanced more effectively by GO-Ag than GO + Ag (simple mixture of GO and AgNPs) due to the synergistical activity of GO and the decorated AgNPs in GO-Ag. It is interesting that the diameter of inhibition zone against *E. coli* is a little bigger than that of *S. aureus* for all the tested membranes although these results were not statistically different. The different responses of Gram-negative *E. coli* and Gram-positive *S. aureus* toward CG-based membranes are believed to be correlated to the different structures and chemical compositions of cell membranes.[67,68]

To further evaluate the effect of incorporated nanofillers on antibacterial performance, the growth kinetics of bacteria was monitored in 10 mL LB broth supplemented with different CG-based nanofiber membranes. As shown in Figure 9(a), the growth curves for all other samples except GO/CG can be divided into three phases: lag phase, exponential phase and stationary phase. For *E. coli*, the lag time of the lag phases is 3 h (control), 4.5 h (CG), 4.5 h (GO/CG), 7.5 h (AgNPs/CG), and 8 h (GO + Ag), respectively. In addition, the optical densities (OD, as an indicator of cell number) in stationary phase are in the following sequence: control < CG < GO/CG < AgNPs/CG < GO + Ag/CG. The longer lag time and lower OD value indicates better antibacterial performance. Thus, all CG-based membranes can effectively impede the growth of *E. coli* and the antibacterial properties of CG can be enhanced by the incorporation of GO or/and AgNPs. Furthermore, OD of *E. coli* maintains a low and constant value during 24 h of culture for GO-Ag/CG, indicating the bacteria growth was strongly inhibited. Thus, the best antibacterial performance against *E. coli* was found on GO-Ag/CG. The growth curves of *S. aureus* were displayed in Figure 9(b). After comparing the lag time and OD values of stabilization phase as shown in Figure 9(a,b), similar sequence on antibacterial performance of CG-based nanofiber membranes was determined. GO-Ag/CG still possessed the optimum antibacterial ability against *S. aureus*. It should be pointed out that the monophase of growth curve for GO-Ag/CG is transformed to the regular three phases when E. coli are substituted by *S. aureus*, confirming that *E. coli* are more sensitive than *S. aureus* to CG-based membranes. All results of bacterial growth kinetics are highly consistent with the data of agar disc diffusion.

CONCLUSIONS

In this work, the potential improvement in the mechanical and antibacterial properties of CG nanofiber membranes with the incorporation of GO-Ag composite fillers was thoroughly exploited. First of all, the successful synthesis of GO-Ag by *in situ* reduction of Ag^+ on the surface of GO sheets was confirmed by TEM, UV–vis, XRD, EDS, and FTIR analysis. The incorporation of GO-Ag nanocomposites can synergistically enhance both mechanical and antibacterial properties of CG composites matrix. The introduction of GO-Ag induces 105% enhancement of the elastic modulus and 488% augment of tensile strength on CG nanofiber membranes. The synergistically enhancement in the mechanical properties on of GO-Ag/CG are partially resulted from the alleviated restacking of graphene sheets by the anchored AgNPs, which is supported by TEM and DSC results. Meanwhile, owing to excellent antibacterial ability of GO-Ag, the diameters of inhibition zone of GO-Ag/CG nanofiber membranes against *E. coli* and *S. aureus* are enlarged by 80.5% and 50.1% on top of that of CG, respectively. The synergistical improvement on antibacterial ability of GO-Ag/CG may involve the accumulation of microorganisms to the vicinity of AgNPs by GO. The incorporation of GO-Ag possesses great potential for simultaneously improving mechanical and antibacterial performance of PEC nanofibers in biomedical applications.

ACKNOWLEDGMENTS

This research was supported by National Natural Science Foundation of China (21571147), Innovative Team Program of the Natural Science Foundation of Hubei Province (2014CFA011), Innovative Team Incubation Program in High-Tech Industry of Wuhan City (2014070504020244), Natural Science Foundation of Hubei Province (2016CFB264, 2015CFB430), Hubei Collaborative Innovation Center for Down-Streaming Products in Ethylene Project and Process Intensification and Graduate Innovative Fund of Wuhan Institute of Technology.

REFERENCES

1. Fang, J.; Zhang, Y.; Yan, S.; Liu, Z.; He, S.; Cui, L.; Yin, J. *Acta Biomater.* **2014**, *10*, 276.
2. Luo, Y.; Wang, Q. *Int. J. Biol. Macromol.* **2014**, *64*, 353.
3. Cai, N.; Han, C.; Luo, X.; Chen, G.; Dai, Q.; Yu, F. *Macromol. Mater. Eng.* **2017**, *302*, 1600364.
4. Qin, Y. H.; Jiang, Y.; Niu, D. F.; Zhang, X. S.; Zhou, X. G.; Niu, L.; Yuan, W. K. *J. Power Sources* **2012**, *215*, 130.
5. Jiang, C.; Wang, Z.; Zhang, X.; Zhu, X.; Nie, J.; Ma, G. *RSC Adv.* **2014**, *4*, 41551.
6. Meng, X.; Perry, S. L.; Schiffman, J. D. *ACS Macro Lett.* **2017**, *6*, 505.
7. Bikiaris, D. N.; Triantafyllidis, K. S. *Mater. Lett.* **2013**, *93*, 1.
8. Liu, L.; Liu, Z.; Bai, H.; Sun, D. D. *Water Res.* **2012**, *46*, 1101.
9. Rujitanaroj, P-o.; Pimpha, N.; Supaphol, P. *Polymer* **2008**, *49*, 4723.
10. Dhivya, S.; Padma, V. V.; Santhini, E. *Biomedicine* **2015**, *5*, 22.
11. Wangkulangkul, P.; Jaipaew, J.; Puttawibul, P.; Meesane, J. *Mater. Des.* **2016**, *106*, 428.
12. Xu, X.; Lü, S.; Gao, C.; Bai, X.; Feng, C.; Gao, N.; Liu, M. *Mater. Des.* **2015**, *88*, 1127.
13. Hegab, H. M.; Zou, L. *J. Membr. Sci.* **2015**, *484*, 95.
14. Zhao, Q.; Hou, J.; Shen, J.; Liu, J.; Zhang, Y. *J. Mater. Chem. A* **2015**, *3*, 18696.
15. Rao, S. S.; Nelson, M. T.; Xue, R.; DeJesus, J. K.; Viapiano, M. S.; Lannutti, J. J.; Sarkar, A.; Winter, J. O. *Biomaterials* **2013**, *34*, 5181.
16. Cai, N.; Li, C.; Han, C.; Luo, X.; Shen, L.; Xue, Y.; Yu, F. *Appl. Surf. Sci.* **2016**, *369*, 492.
17. Cai, N.; Hou, D.; Luo, X.; Han, C.; Fu, J.; Zeng, H.; Yu, F. *Compos. Sci. Technol.* **2016**, *135*, 128.
18. Cai, N.; Dai, Q.; Wang, Z.; Luo, X.; Xue, Y.; Yu, F. *Fiber Polym.* **2014**, *15*, 2544.
19. Coleman, J. N.; Khan, U.; Blau, W. J.; Gun'ko, Y. K. *Carbon* **2006**, *44*, 1624.
20. Qi, R.; Guo, R.; Shen, M.; Cao, X.; Zhang, L.; Xu, J.; Yu, J.; Shi, X. *J. Mater. Chem.* **2010**, *20*, 10622.
21. Buschle-Diller, G.; Cooper, J.; Xie, Z.; Wu, Y.; Waldrup, J.; Ren, X. *Cellulose* **2007**, *14*, 553.
22. Kim, K.; Luu, Y. K.; Chang, C.; Fang, D.; Hsiao, B. S.; Chu, B.; Hadjiargyrou, M. *J. Controlled Release* **2004**, *98*, 47.
23. Marambio-Jones, C.; Hoek, E. M. *J. Nanoparticle Res.* **2010**, *12*, 1531.
24. Dai, K.; Shi, L.; Fang, J.; Zhang, Y. *Mater. Sci. Eng. A* **2007**, *465*, 283.
25. Liu, H. H.; Li, Q.; Liang, X.; Xiong, X.; Yu, J.; Guo, Z. X. *J. Appl. Polym. Sci.* **2016**, *133*, 43850.
26. Hu, W.; Peng, C.; Luo, W.; Lv, M.; Li, X.; Li, D.; Huang, Q.; Fan, C. *ACS Nano* **2010**, *4*, 4317.
27. Yin, S.; Goldovsky, Y.; Herzberg, M.; Liu, L.; Sun, H.; Zhang, Y.; Meng, F.; Cao, X.; Sun, D. D.; Chen, H. *Adv. Funct. Mater.* **2013**, *23*, 2972.
28. Tang, J.; Chen, Q.; Xu, L.; Zhang, S.; Feng, L.; Cheng, L.; Xu, H.; Liu, Z.; Peng, R. *ACS Appl. Mater. Interfaces* **2013**, *5*, 3867.
29. Shen, J.; Shi, M.; Li, N.; Yan, B.; Ma, H.; Hu, Y.; Ye, M. *Nano Res.* **2010**, *3*, 339.
30. Kumar, S.; Raj, S.; Jain, S.; Chatterjee, K. *Mater. Des.* **2016**, *108*, 319.
31. Marcano, D. C.; Kosynkin, D. V.; Berlin, J. M.; Sinitskii, A.; Sun, Z.; Slesarev, A.; Alemany, L. B.; Lu, W.; Tour, J. M. *ACS Nano* **2010**, *4*, 4806.
32. Sun, X.-F.; Qin, J.; Xia, P.-F.; Guo, B.-B.; Yang, C.-M.; Song, C.; Wang, S. G. *Chem. Eng. J.* **2015**, *281*, 53.
33. Das, M. R.; Sarma, R. K.; Saikia, R.; Kale, V. S.; Shelke, M. V.; Sengupta, P. *Colloid Surf. B* **2011**, *83*, 16.
34. Peng, S.; McMahon, J. M.; Schatz, G. C.; Gray, S. K.; Sun, Y. *Proc. Natl. Acad. Sci. USA* **2010**, *107*, 14530.
35. Li, C.; Wang, X.; Chen, F.; Zhang, C.; Zhi, X.; Wang, K.; Cui, D. *Biomaterials* **2013**, *34*, 3882.
36. Ikhsan, N. I.; Rameshkumar, P.; Pandikumar, A.; Mehmood Shahid, M.; Huang, N. M.; Vijay Kumar, S.; Lim, H. N. *Talanta* **2015**, *144*, 908.
37. Dutta, S.; Ray, C.; Sarkar, S.; Pradhan,8 M.; Negishi, Y.; Pal, T. *ACS Appl. Mater. Interfaces* **2013**, *5*, 8724.
38. Belay, M.; Nagarale, R. K.; Verma, V. *J. Appl. Polym. Sci.* **2017**, *134*, 45085.
39. Hui, K.; Hui, K.; Dinh, D.; Tsang, C.; Cho, Y.; Zhou, W.; Hong, X.; Chun, H.-H. *Acta Mater.* **2014**, *64*, 326.
40. Zhang, Z.; Chen, H.; Xing, C.; Guo, M.; Xu, F.; Wang, X.; Gruber, H. J.; Zhang, B.; Tang, J. *Nano Res.* **2011**, *4*, 599.
41. Greiner, A.; Wendorff, J. H. *Angew. Chem. Int. Ed.* **2007**, *46*, 5670.
42. Koosha, M.; Mirzadeh, H.; Shokrgozar, M. A.; Farokhi, M. *RSC Adv.* **2015**, *5*, 10479.
43. Liu, Y.; Park, M.; Shin, H. K.; Pant, B.; Choi, J.; Park, Y. W.; Lee, J. Y.; Park, S.-J.; Kim, H. Y. *J. Ind. Eng. Chem.* **2014**, *20*, 4415.
44. Cai, N.; Li, C.; Luo, X.; Xue, Y.; Shen, L.; Yu, F. *J. Mater. Sci.* **2016**, *51*, 797.
45. Han, Y.; Lu, Y. *Compos. Sci. Technol.* **2009**, *69*, 1231.
46. Kalambate, P. K.; Dar, R. A.; Karna, S. P.; Srivastava, A. K. *J. Power Sources* **2015**, *276*, 262.

47. Shanmugasundaram, N.; Ravichandran, P.; Reddy, P. N.; Ramamurty, N.; Pal, S.; Rao, K. P. *Biomaterials* **2001**, *22*, 1943.
48. Wang, X.; Wang, X.; Tan, Y.; Zhang, B.; Gu, Z.; Li, X. *J. Biomed. Mater. Res. A* **2009**, *89*, 1079.
49. Chen, Z. G.; Wang, P. W.; Wei, B.; Mo, X. M.; Cui, F. Z. *Acta Biomater.* **2010**, *6*, 372.
50. Ke, H.; Pang, Z.; Xu, Y.; Chen, X.; Fu, J.; Cai, Y.; Huang, F.; Wei, Q. *J. Therm. Anal. Calorim.* **2014**, *117*, 109.
51. Cacciotti, I.; Fortunati, E.; Puglia, D.; Kenny, J. M.; Nanni, F. *Carbohydr. Polym.* **2014**, *103*, 22.
52. Wei, J.; Vo, T.; Inam, F. *RSC Adv.* **2015**, *5*, 73510.
53. Wang, C.; Wu, H.; Qu, F.; Liang, H.; Niu, X.; Li, G. *J. Appl. Polym. Sci.* **2016**, *133*, 43417.
54. Cai, N.; Dai, Q.; Wang, Z.; Luo, X.; Xue, Y.; Yu, F. *J. Mater. Sci.* **2015**, *50*, 1435.
55. Wu, J.-K.; Ye, C.-C.; Liu, T.; An, Q.-F.; Song, Y.-H.; Lee, K.-R.; Hung, W.-S.; Gao, C. *J. Mater. Des.* **2017**, *119*, 38.
56. Huang, Y.; Wang, T.; Zhao, X.; Wang, X.; Zhou, L.; Yang, Y.; Liao, F.; Ju, Y. *J. Chem. Technol. Biotechnol.* **2015**, *90*, 1677.
57. Usman, A.; Hussain, Z.; Riaz, A.; Khan, A. N. *Carbohydr. Polym.* **2016**, *153*, 592.
58. Jayakumar, R.; Menon, D.; Manzoor, K.; Nair, S. V.; Tamura, H. *Carbohydr. Polym.* **2010**, *82*, 227.
59. Chen, C.-S.; Liau, W.-Y.; Tsai, G.-J. *J. Food Protect.* **1998**, *61*, 1124.
60. Akhavan, O.; Ghaderi, E. *ACS Nano* **2010**, *4*, 5731.
61. Perreault, F.; de Faria, A. F.; Nejati, S.; Elimelech, M. *ACS Nano* **2015**, *9*, 7226.
62. Cai, X.; Lin, M.; Tan, S.; Mai, W.; Zhang, Y.; Liang, Z.; Lin, Z.; Zhang, X. *Carbon* **2012**, *50*, 3407.
63. Kurantowicz, N.; Sawosz, E.; Jaworski, S.; Kutwin, M.; Strojny, B.; Wierzbicki, M.; Szeliga, J.; Hotowy, A.; Lipińska, L.; Koziński, R.; Jagiełło, J.; Chwalibog, A. *Nanoscale Res. Lett.* **2015**, *10*, 23.
64. de Faria, A. F.; Martinez, D. S. T.; Meira, S. M. M.; de Moraes, A. C. M.; Brandelli, A.; Souza Filho, A. G.; Alves, O. L. *Colloid Surf. B* **2014**, *113*, 115.
65. Shao, W.; Liu, X.; Min, H.; Dong, G.; Feng, Q.; Zuo, S. *ACS Appl. Mater. Interfaces* **2015**, *7*, 6966.
66. Liu, S.; Hu, M.; Zeng, T. H.; Wu, R.; Jiang, R.; Wei, J.; Wang, L.; Kong, J.; Chen, Y. *Langmuir* **2012**, *28*, 12364.
67. Morones, J. R.; Elechiguerra, J. L.; Camacho, A.; Holt, K.; Kouri, J. B.; Ramírez, J. T.; Yacaman, M. J. *Nanotechnology* **2005**, *16*, 2346.
68. Shrivastava, S.; Bera, T.; Roy, A.; Singh, G.; Ramachandrarao, P.; Dash, D. *Nanotechnology* **2007**, *18*, 225103.